

# Data-driven Discovery of Pt Single Atom Embedded Germanosilicate MFI Zeolite Catalysts for Propane Dehydrogenation

Qian-Cheng Zhao,<sup>1</sup> Lin Chen,<sup>1</sup> Sicong Ma<sup>2\*</sup> and Zhi-Pan Liu<sup>1,2\*</sup>

<sup>1</sup> Shanghai Key Laboratory of Molecular Catalysis and Innovative Materials, Key Laboratory of Computational Physical Science, Department of Chemistry, Fudan University, Shanghai 200433, China

<sup>2</sup> State Key Laboratory of Metal Organic Chemistry, Shanghai Institute of Organic Chemistry, Chinese Academy of Sciences, Shanghai 200032, China

Corresponding Author: \*scma@mail.sioc.ac.cn; \*zpliu@fudan.edu.cn

## Table of contents

1. Supplementary Methods
2. Table S1-S3
3. Figure S1-S17
4. Supplementary References

## Supplementary Methods

**Synthesis of Pt@Ge-MFI zeolites:** The Pt precursor solution was first prepared by mixing 1.2 g  $\text{H}_2\text{PtCl}_6 \cdot x\text{H}_2\text{O}$ , 14 mL ethylenediamine (EDA) and 160 mL deionized water followed by overnight stirring. Then, Pt@Ge-MFI zeolite was prepared by a one-pot synthesis strategy. 16.48 g tetraethyl orthosilicate, 20 g deionized water and demanded amount of germanium oxide was added into 25.98 g tetrapropylammonium solution (25 wt% in water, TPAOH). The resultant solution was stirred for 3 hours (500 rpm) at ambient temperature before 8.5 mL Pt precursor solution was added. After an additional 10 minutes of stirring, the solution was transferred into a 100 mL Teflon-lined autoclave. Afterwards, the hydrothermal synthesis was carried out at 170 °C for 96 hours in an electric oven. The as-synthesized raw product, Pt@Ge-MFI(r), obtained by filtration, wash and overnight drying at 80 °C, was then loaded in the fixed-bed reactor for catalytic tests, where the catalyst was pre-reduced as Pt@Ge-MFI. In the meantime, Pt@Ge-MFI(r) was calcined in a muffle furnace at 873 K for 4 h followed by 4 hours'  $\text{H}_2$  reduction to make Pt@Ge-MFI-c. The Pt@Ge-MFI(s) was obtained from Pt@Ge-MFI after pre-reduction and direct 12 hours' propane dehydrogenation (PDH) reaction at 873 K. Similarly, Pt@Ge-MFI-c(s) was obtained from Pt@Ge-MFI-c after pre-reduction and reaction as well.

Furthermore, a control catalyst without Ge doping was synthesized using the same procedure as Pt@Ge-MFI, and was referred to as Pt@MFI.

**Synthesis of Ge-IWW zeolites:** The OSDA utilized for IWW was 1,4-bis-(dimethyl-1-adamantylammonium)-butane, whose synthesis were reported by Lu K. et al.<sup>1</sup> The synthesis gel had an overall molar ratio of Si: Ge: OSDA:  $\text{H}_2\text{O}$  = 1: 0.5 : 0.3 : 20. The gel was stirred for 3 hours (500 rpm) at ambient temperature before transferred to a 50 mL Teflon-lined autoclave. Afterwards, the hydrothermal synthesis was carried out at 175 °C for 72 hours in an electric oven. The product was washed and dried at 80 °C. The XRD patterns were collected subsequently for analysis.

**Synthesis of Pt@Ge-IWW zeolites (unsuccessful):** The trial for Pt@Ge-IWW synthesis followed the same protocol as that for Ge-IWW, except that Pt precursor solution was added to the synthesis gel before stirring and hydrothermal synthesis. However, the XRD pattern of the resulting product could not match any known zeolites.

**Catalyst characterization:** Powdered X-ray diffraction (PXRD) patterns were obtained on a Bruker D8 using Cu ( $K\alpha = 0.15406$  nm) as the X-ray source. X-ray photoelectron spectroscopy (XPS) measurements were performed on AXIS Kratos Supra+. High-resolution transmission electron microscopy (HR-TEM) data were obtained on an FEI Tecnai G2 F20 S-TWIN transmission electron microscopy instrument operating at 200 kV. Scanning electron microscopy (SEM) images were taken by a Hitachi Scanning Electron Microscope Flex SEM 1000. The element content of various catalysts was performed by ICP-MS with an Agilent 7800 (MS) instrument.

**In situ XRD:** In situ XRD was performed with a Dandong Tongda instrument using Cu ( $K\alpha = 0.15406$  nm) as the X-ray source. The in-situ cell was purged with air (30 sccm) or  $\text{H}_2$  (30 sccm) for 1 hour after the sample was loaded. Then the XRD patterns were obtained at 303 K, 373 K, 473 K, 573 K, 673 K, 773 K, 823 K, 873 K, and at 873 K after 4 hours' treatment.

**CO-DRIFT:** CO-DRIFT experiments were conducted on a NICOLET iS50 FT-IR spectrometer, covering the range from 4000 to 650  $\text{cm}^{-1}$ . Initially, the sample was ground thoroughly and loaded into the in-situ reaction cell. Subsequently, the sample was pre-treated in 10 sccm  $\text{H}_2$  at 673 K for 1 hour and cooled down to room temperature in 30 sccm He flow before the background was collected. Then 5

sccm CO flow was slowly introduced into the cell for 1 hour, He purge was switched for another 1 hour, and the spectra were collected.

**XAFS:** Pt L3-edge analysis was performed with Si(111) crystal monochromators at the BL11B beamlines at the Shanghai Synchrotron Radiation Facility (SSRF) (Shanghai, China). Before the analysis at the beamline, samples were pressed into thin sheets with 1 cm in diameter and sealed using Kapton tape film. The XAFS spectra were recorded at room temperature using a 4-channel Silicon Drift Detector (SDD) Bruker 5040. Pt L3-edge extended X-ray absorption fine structure (EXAFS) spectra were recorded in transmission mode. Negligible changes in the line-shape and peak position of Pt L3-edge XANES spectra were observed between two scans taken for a specific sample. The XAFS spectra of standard samples including Pt foil and PtO<sub>2</sub> were recorded in transmission mode. Data reduction, data analysis, and EXAFS fitting were performed and analyzed with the Athena and Artemis programs of the Demeter data analysis packages that utilized the FEFF6 program to fit the EXAFS data.<sup>2,3</sup> The energy calibration of the sample was conducted through standard and Pt foil, which as a reference was simultaneously measured. A linear function was subtracted from the pre-edge region, then the edge jump was normalized using Athena software. The  $\chi(k)$  data were isolated by subtracting a smooth, third-order polynomial approximating the absorption background of an isolated atom. The  $k^2$ -weighted  $\chi(k)$  data were Fourier transformed after applying a HanFeng window function ( $\Delta k = 1.0$ ). For EXAFS modeling, the global amplitude EXAFS (CN,  $R$ ,  $\sigma^2$  and  $\Delta E_0$ ) were obtained by nonlinear fitting, with least-squares refinement, of the EXAFS equation to the Fourier-transformed data in R-space, using Artemis software, EXAFS of the Pt foil were fitted and the obtained amplitude reduction factor  $S_0^2$  value (0.82) was set in the EXAFS analysis to determine the coordination numbers (CNs) in sample.

**Table S1.** Zeolite screening for Ge replacement, propane and propene diffusion and Pt species introduction.

	zeocode	$\Delta E_{rep}^a$	rings	Include Sphere <sup>b</sup>	Diffuse sphere <sup>c</sup>	$\Delta E_{Pt1}^d$	$\Delta E_{Pt4}^e$
0	NON	0.15	[6, 5, 4]	6.5	[2.27, 2.3, 2.3]		
1	NPT	0.16	[8, 4, 3]	10.28	[3.56, 3.56, 3.56]		
2	OBW	0.09	[10, 8, 4, 3]	9.26	[5.18, 5.18, 3.62]	-0.25	-1.16
3	OKO	-0.31	[12, 10, 6, 5, 4]	6.7	[1.34, 5.1, 5.9]	0.49	-0.16
4	OWE	0.37	[8, 6, 4]	5.78	[3.79, 3.6, 1.82]		
5	PHI	0.38	[8, 4]	5.4	[3.69, 3.11, 3.31]		
6	POS	0.30	[12, 11, 6, 5, 4]	7.27	[5.68, 5.68, 6.58]	-0.36	-0.69
7	PWO	0.27	[9, 5, 4]	5.22	[1.33, 4.35, 4.35]	-0.17	-1.18
8	OSI	-0.10	[12, 6, 4]	6.66	[2.44, 2.44, 6.28]		
9	PCR	0.31	[12, 10, 8, 6, 5]	6.03	[1.51, 3.16, 4.2]		
10	PON	0.29	[10, 6, 4]	4.93	[4.3, 1.97, 2.21]		
11	PSI	0.39	[10, 8, 6, 4]	5.79	[4.85, 1.73, 1.84]		
12	PWW	0.25	[10, 8, 5, 4]	5.23	[1.55, 2.91, 4.85]		
13	ABW	0.26	[8, 6, 4]	4.24	[2.61, 3.51, 2.61]		
14	AEI	0.30	[8, 6, 4]	7.33	[3.84, 3.84, 3.64]		
15	AEL	0.39	[10, 6, 4]	5.64	[4.63, 2.01, 2.01]		
16	AEN	-0.67	[8, 6, 4]	4.43	[1.21, 3.38, 3.66]		
17	AET	0.09	[14, 6, 4]	8.41	[1.78, 1.78, 7.59]		
18	AFG	0.25	[6, 4]	6.37	[2.55, 2.55, 2.54]		
19	AFI	0.27	[12, 6, 4]	8.3	[2.22, 2.22, 7.42]		
20	AFN	0.31	[8, 6, 4]	5.25	[2.85, 2.53, 2.85]		
21	AFO	0.31	[10, 6, 4]	5.43	[2.21, 1.49, 5.07]		
22	AFR	0.22	[12, 8, 6, 4]	8.36	[1.64, 3.77, 6.97]		
23	AFS	0.24	[12, 8, 6, 4]	9.51	[3.76, 3.76, 6.01]		
24	AFT	0.38	[8, 6, 4]	7.75	[3.68, 3.68, 3.68]		
25	AFV	0.22	[8, 6, 4]	7.08	[3.46, 3.46, 2.48]		
26	AFX	0.38	[8, 6, 4]	7.76	[3.73, 3.73, 3.73]		
27	AFY	0.32	[12, 8, 4]	7.82	[4.08, 4.08, 5.9]	-0.27	-1.23
28	AHT	-0.30	[10, 6, 4]	3.95	[2.4, 2.4, 2.75]		
29	ANA	0.26	[8, 6, 4]	4.21	[2.43, 2.43, 2.43]		
30	APC	0.39	[8, 6, 4]	4.23	[3.16, 2.57, 2.6]		
31	APD	0.36	[8, 6, 4]	4.93	[3.63, 2.45, 2.68]		
32	AST	0.42	[6, 4]	7.94	[1.91, 1.91, 1.91]		
33	ASV	0.30	[12, 6, 4]	5.43	[1.52, 1.52, 4.43]		
34	ATN	0.46	[8, 6, 4]	5.91	[1.94, 1.94, 4.11]		
35	ATO	0.36	[12, 6, 4]	5.74	[2.12, 2.12, 5.49]		
36	ATS	0.37	[12, 6, 4]	7.3	[2.44, 1.62, 6.82]		
37	ATT	0.29	[8, 6, 4]	5.42	[3.79, 3.69, 1.41]		
38	ATV	0.18	[8, 6, 4]	4.74	[3.48, 2.39, 2.14]		
39	AVL	0.25	[8, 6, 4]	7.14	[3.55, 3.55, 2.48]		
40	AWO	0.35	[8, 6, 4]	5.16	[3.67, 3.04, 1.89]		

41	AWW	0.32	[8, 6, 4]	7.48	[1.86, 1.86, 4.17]		
42	BCT	-0.14	[8, 6, 4]	3.8	[2.55, 2.55, 2.91]		
43	BEA	0.35	[12, 6, 5, 4]	6.68	[5.95, 5.95, 5.95]		
44	BEC	0.26	[12, 6, 5, 4]	6.95	[6.09, 6.09, 6.09]	-0.25	-1.29
45	BIK	0.49	[8, 6, 5]	4.17	[2.55, 1.56, 3.55]		
46	BOF	0.13	[10, 6, 5, 4]	5.58	[4.67, 1.77, 1.77]		
47	BOG	0.22	[12, 10, 6, 5, 4]	8.05	[6.88, 4.92, 4.92]	-0.18	-0.57
48	BOZ	0.12	[10, 8, 6, 4, 3]	8.71	[4.92, 3.68, 4.92]	1.15	-1.17
49	BPH	0.25	[12, 8, 6, 4]	9.51	[3.51, 3.51, 6.01]		
50	BRE	0.12	[8, 6, 5, 4]	5.29	[2.74, 1.64, 2.96]		
51	BSV	0.10	[12, 6, 4]	5.17	[3.84, 3.84, 3.84]		
52	CAN	0.38	[12, 6, 4]	6.27	[2.53, 2.53, 5.96]		
53	CAS	0.21	[8, 6, 5]	5.05	[2.97, 2.21, 2.45]		
54	CDO	-0.38	[8, 5]	5.78	[3.44, 1.52, 3.35]		
55	CFI	0.32	[14, 6, 5, 4]	7.47	[2.62, 7.26, 2.4]		
56	CGF	0.06	[10, 8, 6, 4]	5.76	[2.29, 1.46, 3.03]		
57	CGS	0.25	[10, 8, 6, 4]	5.86	[4.01, 2.97, 2.97]		
58	CHA	0.28	[8, 6, 4]	7.37	[3.72, 3.72, 3.72]		
59	CSV	0.25	[10, 8, 6, 5, 4]	7.56	[1.72, 3.28, 5.31]		
60	CTH	-0.40	[14, 10, 6, 5, 4]	8.14	[7.45, 3.92, 2.22]		
61	CZP	0.08	[12, 8, 4]	4.26	[1.25, 1.25, 3.68]		
62	DAC	0.33	[10, 8, 5, 4]	5.28	[1.57, 4.19, 3.66]		
63	DDR	0.34	[8, 6, 5, 4]	7.66	[3.65, 3.65, 2.63]		
64	DFO	0.11	[12, 10, 8, 6, 4]	11.29	[5.08, 5.08, 7.19]		
65	DFT	0.47	[8, 6, 4]	5.1	[3.07, 3.07, 3.65]		
66	DOH	-0.06	[6, 5, 4]	7.85	[2.55, 2.55, 2.62]		
67	DON	0.10	[14, 6, 5, 4]	8.79	[2.19, 1.79, 8.07]		
68	EAB	0.34	[8, 6, 4]	7.14	[3.54, 3.54, 2.5]		
69	EDI	0.33	[8, 4]	5.72	[3.2, 3.2, 3.44]		
70	EEI	-0.15	[8, 6, 5, 4]	6.96	[3.11, 2.15, 2.23]		
71	EMT	0.06	[12, 6, 4]	11.55	[6.54, 6.54, 7.37]		
72	EON	0.29	[12, 8, 6, 5, 4]	7.83	[6.79, 3.24, 1.9]		
73	EPI	0.32	[8, 5, 4]	5.47	[3.62, 1.25, 3.48]		
74	ERI	0.19	[8, 6, 4]	7.04	[3.42, 3.42, 3.42]		
75	ESV	0.31	[8, 6, 5, 4]	6.22	[1.78, 3.66, 1.78]		
76	ETL	0.31	[8, 6, 5, 4]	6.37	[3.19, 1.63, 3.42]		
77	ETR	0.21	[18, 8, 6, 4]	10.05	[2.85, 2.85, 9.33]		
78	EUO	0.11	[10, 6, 5, 4]	7	[4.99, 1.98, 2.5]		
79	EWS	0.23	[10, 6, 5, 4]	6.12	[1.94, 3.99, 3.99]		
80	EZT	0.21	[12, 8, 6, 4]	6.57	[6.13, 2.12, 2.12]		
81	FAR	0.38	[6, 4]	6.36	[2.47, 2.47, 2.26]		
82	FAU	0.30	[12, 6, 4]	11.24	[7.35, 7.35, 7.35]		

83	FER	0.39	[10, 8, 6, 5]	6.31	[1.56, 3.4, 4.69]		
84	FRA	0.53	[6, 4]	6.67	[2.7, 2.7, 2.66]		
85	GME	0.36	[12, 8, 6, 4]	7.76	[3.41, 3.41, 7.11]		
86	GON	0.36	[12, 6, 5, 4]	6.32	[1.68, 1.68, 5.45]		
87	GOO	0.14	[8, 6, 4]	4.51	[3.22, 3.22, 2.84]		
88	HEU	0.32	[10, 8, 5, 4]	5.97	[3.05, 1.34, 3.67]		
89	IFO	0.10	[16, 6, 4]	7.76	[7.22, 1.97, 1.09]		
90	IFR	0.19	[12, 6, 5, 4]	7.24	[1.64, 1.3, 6.38]		
91	IFW	0.25	[10, 8, 6, 5, 4]	7.7	[3.28, 3.28, 5.63]		
92	IFY	0.21	[8, 6, 4]	6.94	[3.83, 3.83, 2.22]		
93	IHW	0.11	[8, 6, 5, 4]	6.67	[3.67, 1.58, 3.67]		
94	IMF	0.26	[10, 6, 5, 4]	7.34	[5.44, 1.84, 5.2]		
95	IRN	0.30	[8, 7, 6, 5, 4]	9.17	[2.05, 3.64, 2.81]		
96	ISV	0.25	[12, 6, 5, 4]	7.01	[6.32, 6.32, 6.28]	-0.28	-1.37
97	ITE	0.31	[8, 6, 5, 4]	8.3	[2.07, 4.21, 2.8]		
98	ITG	0.26	[12, 10, 6, 5, 4]	7	[5.0, 6.3, 5.21]	-0.10	-1.53
99	ITH	0.30	[10, 9, 6, 5, 4]	6.72	[3.53, 5.13, 4.99]	-0.28	-1.41
100	ITR	0.28	[10, 9, 6, 5, 4]	6.36	[5.12, 5.12, 3.58]	-0.15	-1.08
101	ITT	0.20	[18, 10, 6, 5, 4, 3]	11.74	[2.29, 2.29, 11.2]		
102	ITW	0.32	[8, 6, 5, 4]	4.73	[2.78, 1.54, 3.95]		
103	IWR	0.25	[12, 10, 6, 5, 4]	7.48	[4.86, 4.86, 5.91]	-0.18	-1.22
104	IWS	0.16	[12, 6, 5, 4]	8.25	[6.38, 6.38, 6.66]	0.13	0.02
105	IWV	-0.44	[12, 6, 5, 4]	8.54	[2.06, 7.03, 7.03]	0.05	-0.63
106	IWW	0.19	[12, 10, 8, 6, 5, 4]	7.07	[4.91, 4.91, 6.25]	-0.12	0.06
107	JBW	0.36	[8, 6, 4]	4.29	[3.72, 2.53, 1.46]		
108	JNT	0.11	[8, 6, 4]	4.72	[1.75, 1.71, 1.75]		
109	JOZ	0.15	[8, 4, 3]	4.92	[3.09, 3.5, 3.09]		
110	JRY	0.27	[10, 6, 4]	4.59	[2.05, 4.4, 1.75]		
111	JSN	0.31	[8, 6, 4]	5.12	[1.59, 2.75, 3.46]		
112	JSR	-0.04	[11, 6, 4, 3]	7.83	[5.05, 5.05, 5.05]		
113	JST	0.14	[10, 6, 3]	5.35	[3.74, 3.74, 3.74]		
114	JSW	0.22	[8, 6, 4]	5.38	[1.92, 2.6, 1.65]		
115	KFI	0.35	[8, 6, 4]	10.67	[4.04, 4.04, 4.04]		
116	LAU	0.18	[10, 6, 4]	6.04	[2.09, 2.09, 4.07]		
117	LEV	0.36	[8, 6, 4]	7.1	[3.53, 3.53, 2.5]		
118	LIO	0.31	[6, 4]	6.05	[2.37, 2.37, 2.29]		
119	LOS	0.37	[6, 4]	6.36	[2.56, 2.56, 2.56]		
120	LOV	0.19	[9, 8, 6, 4, 3]	5.15	[3.78, 3.78, 3.77]		
121	LTA	0.39	[8, 6, 4]	11.05	[4.21, 4.21, 4.21]		

122	LTF	0.29	[12, 8, 6, 5, 4]	8.16	[3.25, 3.25, 7.5]		
123	LTJ	0.29	[8, 6, 4]	4.1	[3.12, 3.12, 3.12]		
124	LTL	0.27	[12, 8, 6, 4]	10.01	[2.08, 2.08, 7.5]		
125	LTN	0.33	[8, 6, 4]	10.13	[2.08, 2.08, 2.08]		
126	MAR	-0.16	[6, 4]	6.35	[2.43, 2.43, 2.43]		
127	MAZ	0.26	[12, 8, 6, 5, 4]	8.09	[3.25, 3.25, 7.5]		
128	MEI	0.30	[12, 7, 5, 4, 3]	8.06	[2.99, 2.99, 6.9]		
129	MEL	0.30	[10, 8, 6, 5, 4]	7.72	[5.19, 5.19, 5.19]		
130	MEP	0.37	[6, 5]	5.49	[1.72, 1.72, 1.72]		
131	MER	0.35	[8, 4]	6.65	[3.12, 3.12, 4.2]		
132	MFI	0.34	[10, 6, 5, 4]	6.36	[4.7, 4.46, 4.46]	-0.19	0.00
133	MFS	0.37	[10, 8, 6, 5, 4]	6.81	[5.37, 3.2, 1.57]		
134	MON	0.47	[8, 5, 4]	4.24	[3.54, 3.54, 3.54]		
135	MOR	0.34	[12, 8, 5, 4]	6.7	[1.57, 2.95, 6.45]		
136	MOZ	0.26	[12, 8, 6, 4]	10.03	[3.42, 3.42, 7.54]		
137	MRE	0.21	[10, 6, 5, 4]	6.36	[5.59, 2.0, 1.81]		
138	MRT	0.28	[8, 6, 4]	5.97	[3.72, 3.79, 1.47]		
139	MSE	0.36	[12, 10, 6, 5, 4]	7.09	[5.0, 5.0, 6.59]	-0.37	-1.14
140	MSO	0.26	[6, 4]	7.23	[2.09, 2.09, 2.09]		
141	MTF	0.34	[8, 6, 5, 4]	6.25	[1.58, 1.49, 4.03]		
142	MTT	0.36	[10, 6, 5]	6.19	[5.07, 2.2, 1.53]		
143	MTW	0.34	[12, 6, 5, 4]	6.08	[1.27, 5.68, 2.41]		
144	MVY	-3.99	[10, 6, 4]	3.76	[2.94, 1.8, 1.27]		
145	MWW	0.27	[10, 6, 5, 4]	9.69	[4.92, 4.92, 2.6]	-0.19	-1.26
146	NAB	0.20	[9, 8, 4, 3]	4.31	[3.57, 3.57, 3.57]		
147	NAT	0.35	[9, 8, 4]	4.52	[2.99, 2.99, 4.38]		
148	NES	-1.62	[10, 6, 5, 4]	7.04	[5.07, 5.07, 2.06]	1.71	0.79
149	NPO	1.40	[12, 6, 3]	4.23	[2.08, 2.08, 3.71]		
150	NSI	0.42	[8, 6, 5]	4.16	[2.6, 3.3, 2.45]		
151	OFF	0.20	[12, 8, 6, 4]	7	[3.43, 3.43, 6.61]		
152	OSO	0.08	[14, 8, 3]	6.07	[3.41, 3.41, 5.87]		
153	PCS	0.11	[12, 10, 8, 6, 5, 4]	6.84	[1.46, 5.08, 6.27]	-0.05	-1.51
154	POR	0.27	[8, 6, 4]	6.14	[3.74, 3.74, 3.43]		
155	PUN	0.19	[12, 10, 8, 4, 3]	5.51	[4.35, 4.35, 3.41]	-0.22	-0.11
156	RHO	0.40	[8, 6, 4]	10.43	[4.06, 4.06, 4.06]		
157	STI	0.28	[10, 8, 6, 5, 4]	6.29	[4.94, 2.96, 1.85]		
158	STT	0.30	[9, 7, 6, 5, 4]	7.04	[2.76, 1.89, 2.76]		
159	SVV	0.50	[6, 5, 4]	6.41	[1.94, 1.62, 1.94]		

160	SZR	0.27	[10, 8, 6, 5, 4]	6.27	[3.32, 3.32, 4.69]		
161	THO	0.32	[8, 4]	5.15	[3.26, 3.0, 3.69]		
162	TON	0.44	[10, 6, 5]	5.71	[2.31, 1.56, 5.11]		
163	TUN	0.31	[10, 8, 6, 5, 4]	8.46	[4.9, 5.39, 4.9]	-0.20	-0.01
164	UFI	0.44	[8, 6, 4]	10.09	[3.89, 3.89, 1.88]		
165	UOS	0.24	[10, 8, 6, 5, 4]	5.85	[2.6, 4.24, 3.05]		
166	UOZ	0.19	[6, 4]	5.43	[1.49, 1.49, 1.32]		
167	UTL	0.21	[14, 12, 6, 5, 4]	9.3	[1.38, 5.77, 7.61]	-0.18	-0.65
168	VET	0.24	[12, 8, 7, 6, 5]	6.39	[1.51, 1.51, 5.98]		
169	VNI	0.12	[8, 5, 4, 3]	4.8	[3.16, 3.16, 2.53]		
170	WEI	0.28	[10, 8, 6, 4, 3]	4.19	[3.43, 3.43, 3.46]		
171	YUG	0.31	[8, 5, 4]	4.49	[3.08, 1.44, 3.12]		
172	RON	-3.04	[12, 10, 6, 4, 3]	5.74	[1.14, 1.14, 5.11]		
173	RRO	0.25	[10, 8, 5, 4]	4.46	[4.09, 1.54, 3.13]		
174	RSN	0.19	[9, 8, 6, 5, 4, 3]	5.15	[3.77, 2.9, 3.77]		
175	RTE	0.36	[8, 6, 5, 4]	7.06	[1.92, 1.82, 3.98]		
176	RTH	0.31	[8, 6, 5, 4]	8.18	[4.14, 1.67, 2.76]		
177	RUT	0.47	[6, 5, 4]	5.96	[1.93, 1.54, 1.93]		
178	RWR	0.25	[8, 6, 5, 4]	4.42	[1.99, 1.99, 1.66]		
179	RWY	-0.08	[12, 8, 3]	14.4	[6.29, 6.29, 6.29]		
180	SAF	0.42	[12, 6, 4]	6.66	[1.96, 1.5, 6.19]		
181	SAO	0.16	[12, 6, 4]	8.64	[6.79, 6.79, 6.79]	-0.02	0.07
182	SAS	0.62	[8, 6, 4]	8.99	[2.02, 2.02, 4.22]		
183	SAT	0.19	[8, 6, 4]	6.84	[3.25, 3.25, 3.25]		
184	SAV	0.31	[8, 6, 4]	8.82	[3.75, 3.75, 4.1]		
185	SBE	0.24	[12, 8, 6, 4]	12.54	[7.27, 7.27, 3.88]		
186	SBN	0.26	[9, 8, 4, 3]	5.06	[3.8, 3.8, 2.65]		
187	SBS	0.12	[12, 8, 6, 4]	11.45	[7.27, 7.27, 5.72]		
188	SBT	0.21	[12, 8, 6, 4]	11.17	[7.34, 7.34, 5.71]		
189	SEW	0.15	[12, 10, 6, 5, 4]	7.35	[5.29, 5.97, 1.92]	-0.13	-1.16
190	SFE	0.37	[12, 6, 5, 4]	6.66	[1.6, 6.29, 1.6]		
191	SFF	0.43	[10, 6, 5, 4]	7.59	[1.63, 1.37, 5.34]		
192	SFG	0.20	[10, 7, 6, 5, 4]	6.96	[4.98, 2.62, 5.38]	-0.11	-0.90
193	SFH	0.38	[14, 6, 5, 4]	7.63	[6.79, 1.5, 1.78]		
194	SFN	0.33	[14, 6, 5, 4]	7.94	[1.65, 6.7, 2.42]		
195	SFO	0.26	[12, 8, 6, 4]	7.92	[1.64, 3.64, 6.95]		
196	SFS	0.23	[12, 10, 6, 5, 4]	7.52	[1.8, 5.92, 4.84]	-0.13	-0.90

197	SFW	0.36	[8, 6, 4]	7.78	[3.65, 3.65, 3.65]		
198	SGT	0.42	[6, 5, 4]	7.74	[2.11, 2.11, 2.11]		
199	SIV	0.39	[8, 4]	5.38	[3.73, 3.31, 3.37]		
200	SOD	0.55	[6, 4]	6.32	[2.53, 2.53, 2.53]		
201	SOF	0.22	[12, 9, 5, 4]	5.14	[4.17, 4.17, 4.42]	-0.28	-1.29
202	SOR	0.23	[12, 8, 6, 5, 4]	7.06	[3.08, 3.08, 6.66]		
203	SOS	0.24	[12, 8, 6, 4, 3]	4.82	[2.92, 4.27, 2.92]		
204	SOV	0.25	[12, 6, 5, 4]	7.25	[6.55, 6.09, 5.74]	-0.20	-1.32
205	SSF	0.29	[12, 6, 5, 4]	7.66	[6.22, 6.22, 2.61]	0.02	-1.28
206	SSY	0.39	[12, 6, 5, 4]	7.1	[1.67, 1.57, 5.75]		
207	STF	0.31	[10, 6, 5, 4]	7.63	[1.57, 1.26, 5.44]		
208	STO	0.44	[12, 6, 5, 4]	6.8	[1.72, 6.09, 2.07]		
209	STW	0.30	[10, 8, 5, 4]	5.43	[3.38, 3.38, 4.88]		
210	SWY	0.17	[8, 6, 4]	7.06	[3.43, 3.43, 3.43]		
211	TER	0.38	[10, 6, 5, 4]	6.94	[5.16, 1.94, 4.74]		
212	TOL	0.42	[6, 4]	6.37	[2.36, 2.36, 2.06]		
213	TSC	0.28	[8, 6, 4]	16.45	[4.08, 4.08, 4.08]		
214	UEI	0.34	[8, 6, 4]	5.6	[1.9, 3.77, 3.15]		
215	UOE	0.19	[10, 8, 6, 5, 4]	4.96	[3.72, 4.43, 3.01]		
216	UOV	0.13	[12, 10, 8, 6, 5, 4]	6.98	[6.44, 5.38, 5.03]	-0.12	-0.43
217	USI	0.23	[12, 10, 6, 4]	6.76	[1.73, 4.04, 6.28]	-0.22	0.00
218	UWY	0.27	[12, 10, 6, 5, 4]	8.78	[4.96, 5.45, 6.11]	-0.18	-1.10
219	VFI	-0.48	[18, 6, 4]	12.03	[2.4, 2.4, 11.39]		
220	VSV	0.18	[9, 8, 5, 4, 3]	4.31	[3.77, 3.77, 2.9]		
221	YFI	0.24	[12, 8, 6, 5, 4]	7.97	[6.18, 6.18, 3.6]	-0.14	-0.08
222	ZON	0.30	[8, 6, 4]	5.83	[2.63, 3.52, 1.58]		

- Replacement energy of the substitution of one Si atom in the pure silica zeolite framework by Ge(OH)<sub>4</sub>.
- Maximum diameter of a sphere that can be included.
- Maximum diameter of a sphere that can diffuse along.
- Relative energy of the single Pt<sub>1</sub> atom embedded in the zeolite framework.
- Relative energy of the Pt<sub>4</sub> cluster confined in the zeolite channel.

**Table S2.** Atomic content of the zeolites obtained from ICP and XPS.

	ICP results			XPS results		
	Si	Ge	Pt	Si	Ge	Pt
<b>Pt@Ge-MFI(r)<sup>a</sup></b>	24.88	1.04	0.03	26.45	5.32	
<b>Pt@Ge-MFI</b>	30.90	1.23	0.04	25.6	5.28	
<b>Pt@Ge-MFI(s)<sup>b</sup></b>	20.96	1.03	0.03	25.52	5.16	0.02
<b>Pt@Ge-MFI-c(r)<sup>a</sup></b>	27.90	1.22	0.03	25.66	5.66	0.09
<b>Pt@Ge-MFI-c</b>	32.78	1.24	0.04	25.99	5.3	0.07
<b>Pt@Ge-MFI-c(s)<sup>b</sup></b>	32.42	1.24	0.04	26.11	5.39	0.04

- a. 'r' refers to raw sample without reduction treatment.  
b. 's' refers to spent sample obtained after 12 hours' PDH reaction at 873K.

**Table S3.** EXAFS fitting parameters at the Pt L3 –edge for various samples.

Sample	Shell	CN <sup>a</sup>	$R(\text{Å})^b$	$\sigma^2(\text{Å}^2)^c$	$\Delta E_0$ (eV) <sup>d</sup>	K- range/Å <sup>-1</sup>	R- range/Å	R factor <sup>e</sup>
Pt foil	Pt-Pt	12*	2.76 ± 0.01	0.0046	7.0	3.0 - 11.5	1.7 - 3.1	0.0020
PtO <sub>2</sub>	Pt-O	5.2*	2.01 ± 0.01	0.0030	11.0	3.0 - 11.0	1.0 - 2.0	0.0045
Pt@Ge- MFI	Pt-O	3.4 ± 0.7	1.98 ± 0.01	0.0030	8.1	3.5 - 9.5	1.0 - 2.0	0.0128
Pt@Ge- MFI-c	Pt-Pt	10.0 ± 2.0	2.81 ± 0.02	0.0052	9.9	3.0 - 10.0	1.0 - 2.7	0.0136

- CN, coordination number;
- $R$ , distance between absorber and backscatter atoms;
- $\sigma^2$ , Debye-Waller factor to account for both thermal and structural disorders;
- $\Delta E_0$ , inner potential correction;
- R factor, the goodness of the fit.

$S_0^2$  was fixed to 0.82, according to the experimental EXAFS fit of Pt foil by fixing CN as the known crystallographic value. A reasonable range of EXAFS fitting parameters:  $0.700 < S_0^2 < 1.000$ ;  $\text{CN} > 0$ ;  $\sigma^2 \text{Å}^2 > 0$ ;  $|\Delta E_0| < 10 \text{ eV}$ ; R factor  $< 0.02$ .

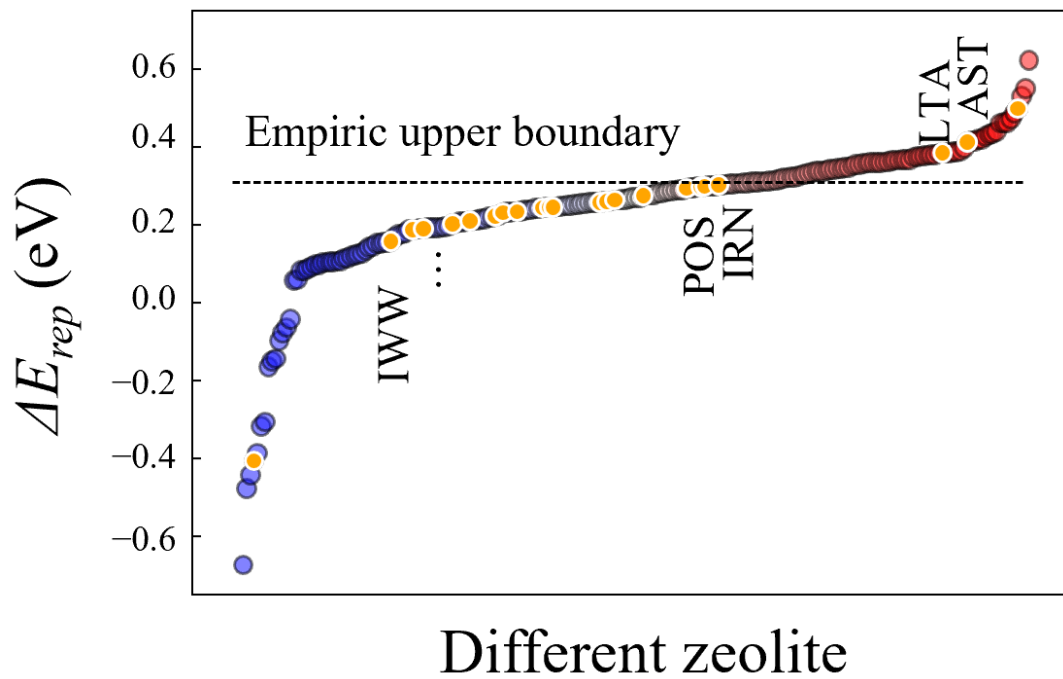


**Figure S1.** The variation of replacement energy of Si by Ge for different zeolite skeletons.

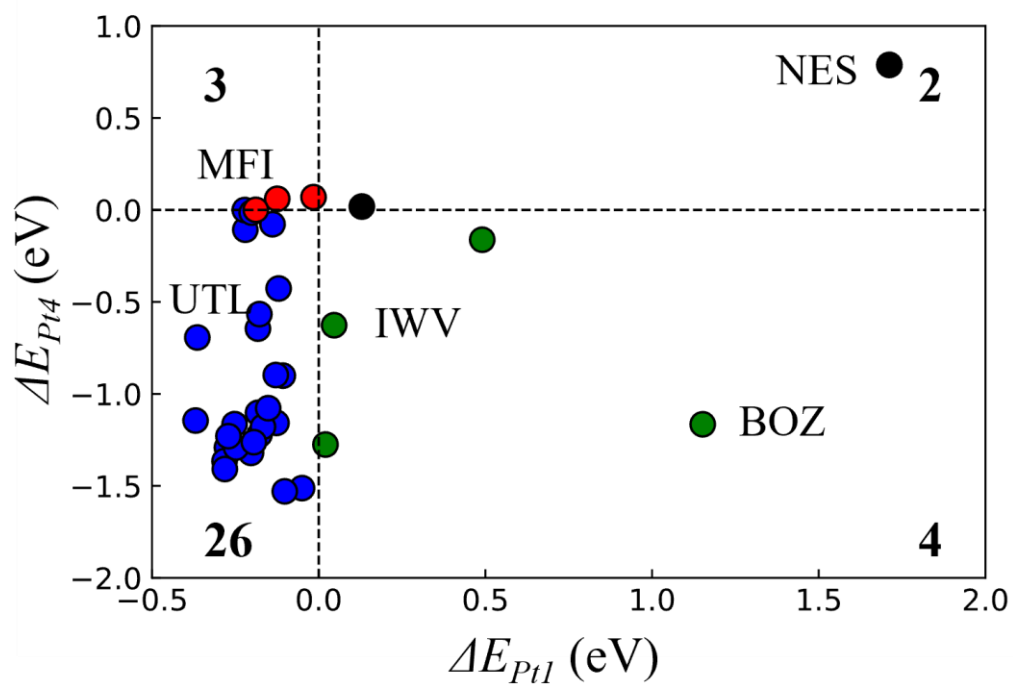


**Figure S2.** The relative stability energy of different Pt existent forms in Ge-doping zeolite compared to the pure silica zeolites, where the x and y axes represent the Pt existence forms of Pt single atom in zeolite skeleton and the Pt<sub>4</sub> cluster in zeolite channel, respectively.

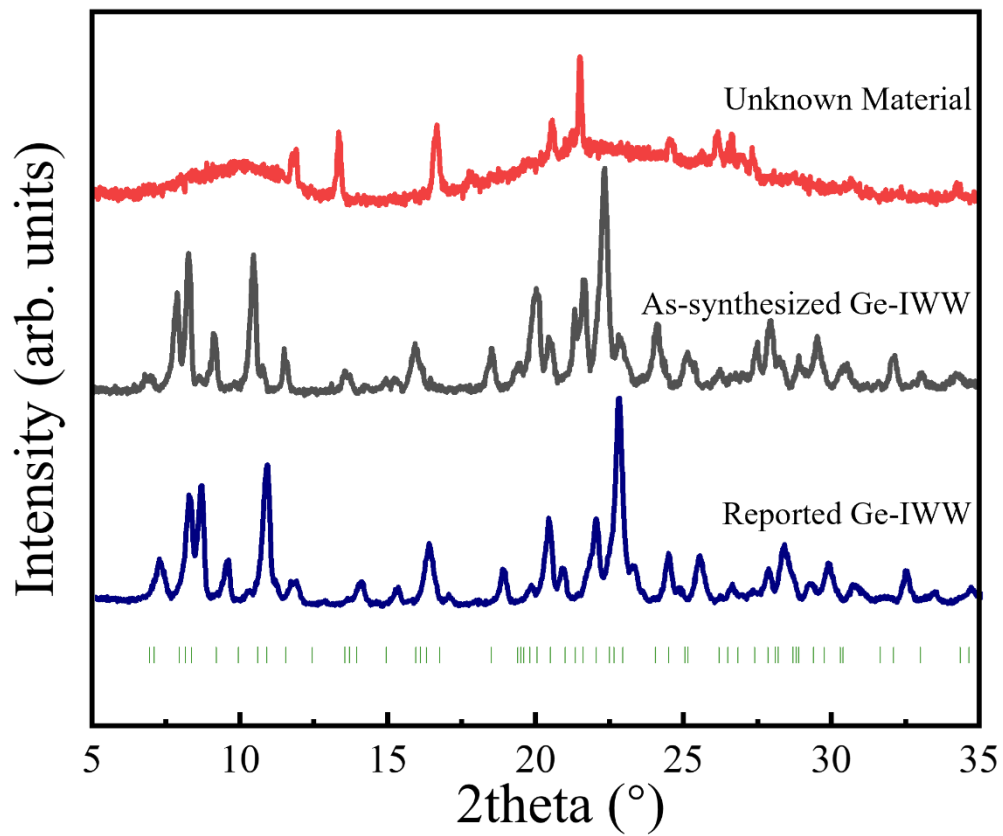


**Figure S3.** XRD patterns of the unknown material obtained from the trial synthesis of Pt@Ge-IWW, as-synthesized Ge-IWW and reported Ge-IWW by Lu K. et al., where the green lines are the calculated peaks of IWW zeolite.<sup>1</sup>

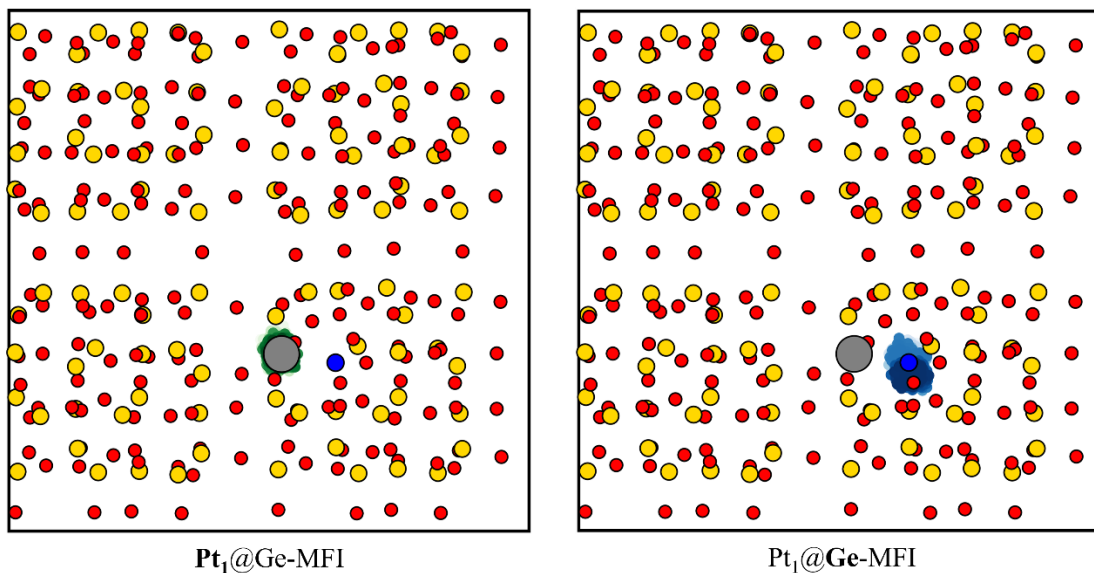


**Figure S4.** The MD trajectories of  $\text{Pt}_1$  single atom and Ge atom embedded in germanosilicate MFI-type zeolite at 873 K. The green and blue color depth indicates the time of appearance of Pt and Ge, respectively. The gray, blue, gold, red and white represent the Pt, Ge, Si, O and H atoms, respectively.

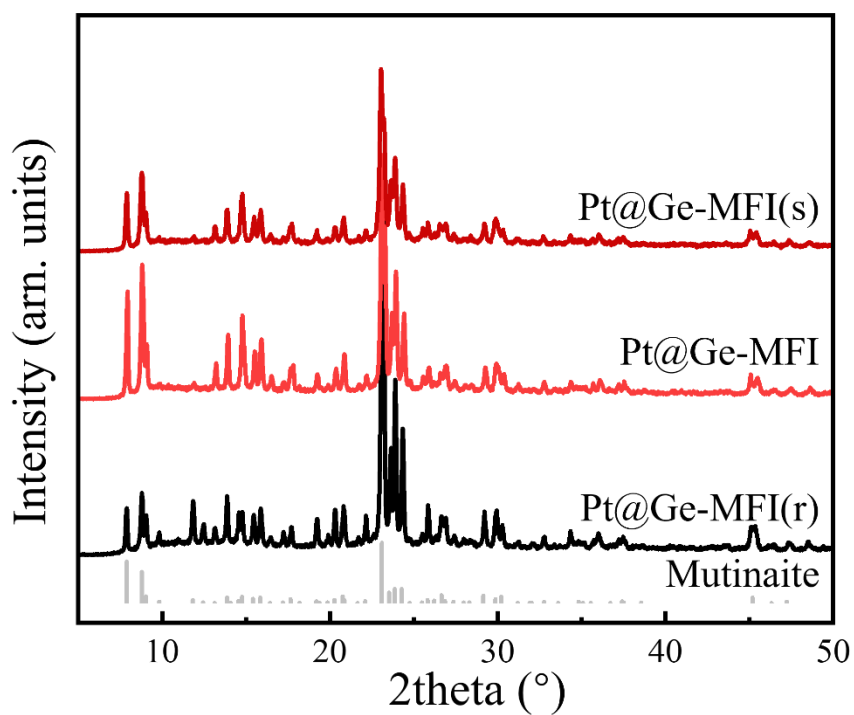


**Figure S5.** XRD patterns of Pt@Ge-MFI(r), Pt@Ge-MFI, Pt@Ge-MFI(s), and standard pattern of Mutinaite (PDF#44-0002), where r refers to the raw sample without H<sub>2</sub> pre-reduction and s refers to the spent sample obtained after 12 hours' PDH reaction at 873 K.

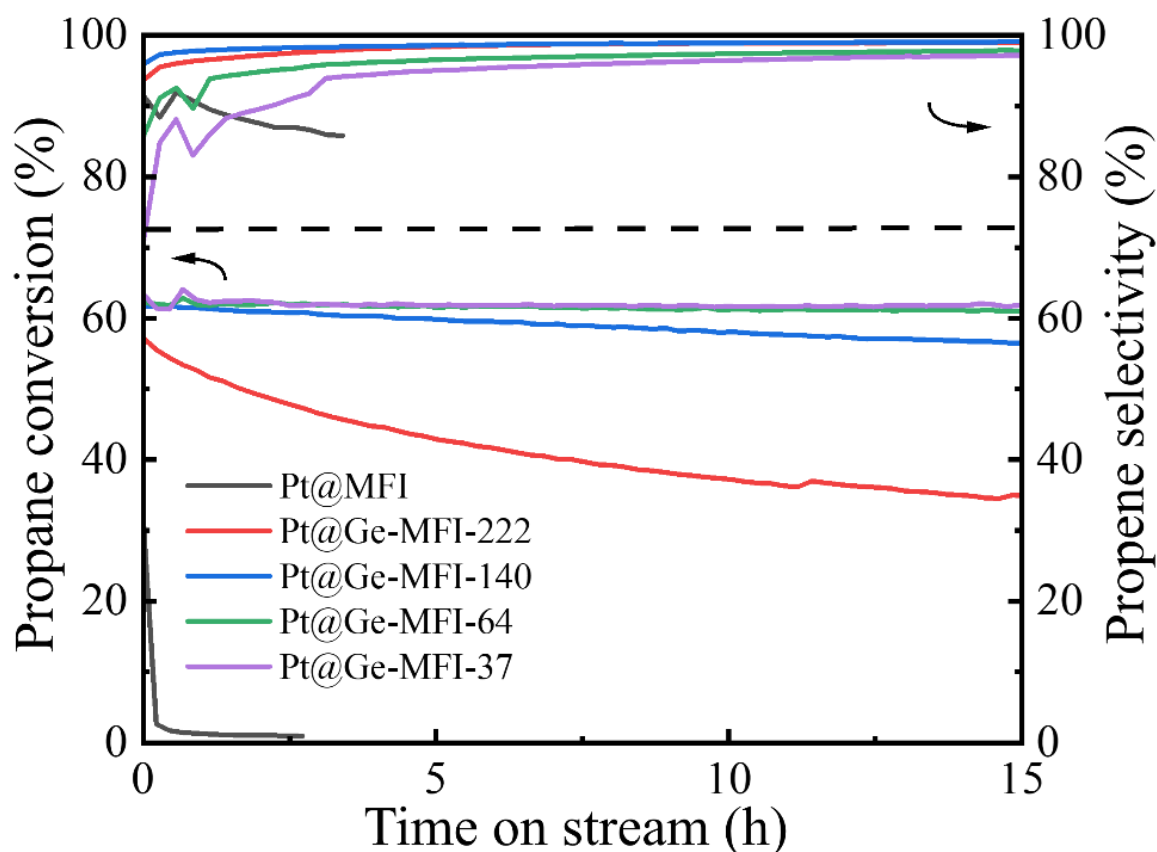


**Figure S6.** The catalytic performance of Pt@Ge-MFI catalysts with various Si:Ge ratios, which are indicated as suffixes in the sample names. The catalysts were pre-treated in H<sub>2</sub> flow for 4 hours, and the PDH reaction was carried out under the condition of  $WHSV_{\text{propane}} = 1.75\text{h}^{-1}$ , propane/N<sub>2</sub> = 1/3, 873 K and atmospheric pressure.

To clarify the effect of Ge content on the catalytic performance, we synthesized a series of samples with different Ge content, as detailed in the Si:Ge ratios and catalytic performance shown in the figure below.

The comparison of catalytic performance between Pt@MFI and Pt@Ge-MFI-222 highlights that a small amount of Ge enhances propane conversion and stability. However, this improvement remains suboptimal. As the Si:Ge ratio decreased to 140, the stability improved, though some deactivation was still evident. Notably, when the Si:Ge ratio was reduced further to 64 and 37, the PDH reaction reached and maintained equilibrium conversion. This suggests that, under a  $WHSV$  of 1.75, the Ge content in Pt@Ge-MFI-64 was sufficient for effectively anchoring Pt.

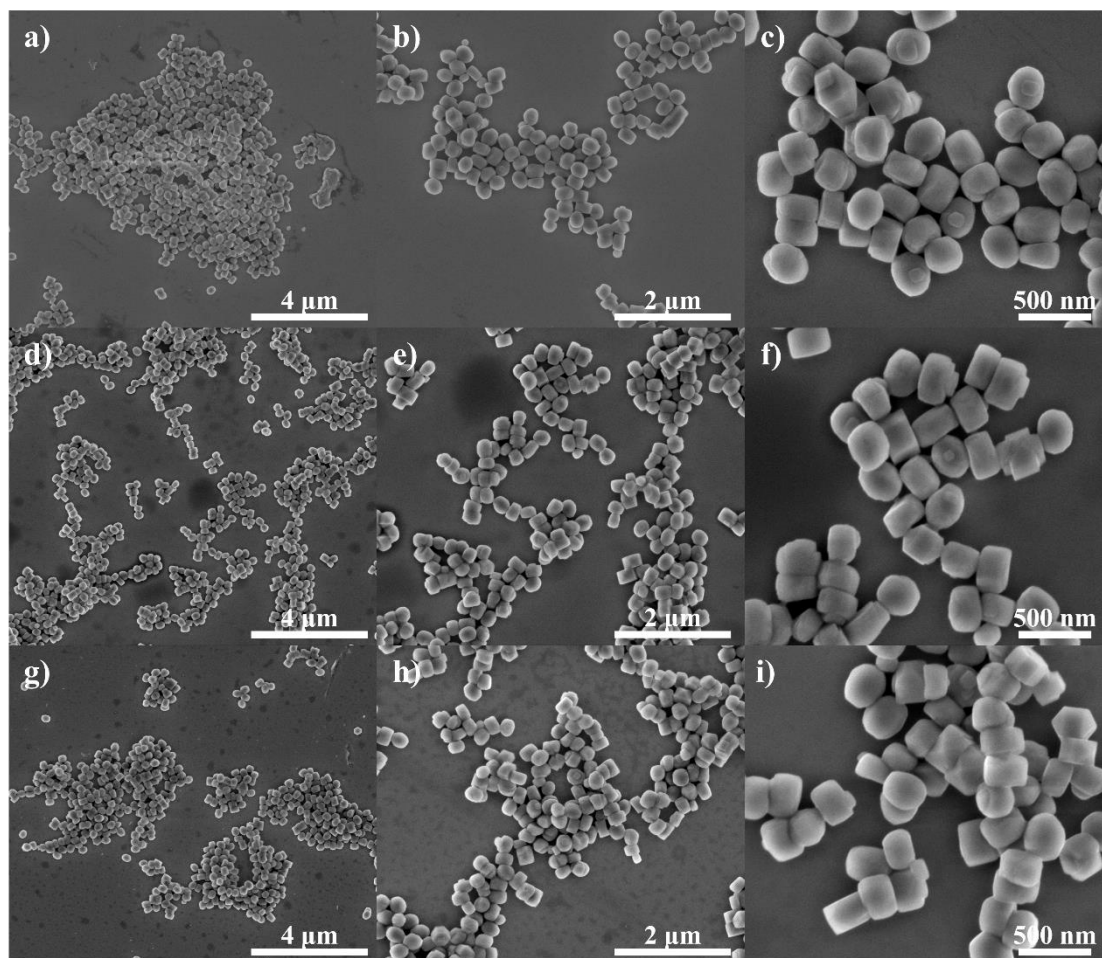


**Figure S7.** SEM images of Pt@Ge-MFI(r) (a-c), Pt@Ge-MFI (d-f) and Pt@Ge-MFI(s) (g-i), where 'r' refers to the raw sample without H<sub>2</sub> pre-reduction and 's' refers to the spent sample obtained after 12 hours' PDH reaction at 873K.

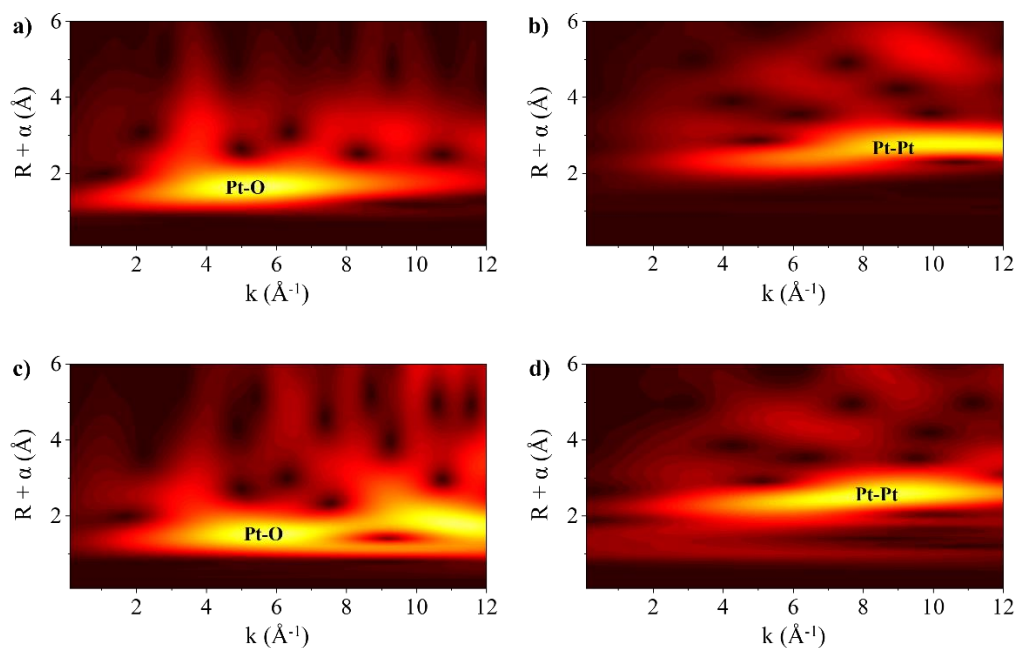


**Figure S8.** WT EXAFS spectra of PtO<sub>2</sub> (a), Pt foil (b), Pt@Ge-MFI (c), Pt@Ge-MFI-c (d). For Wavelet Transform analysis, the  $\chi(k)$  exported from Athena was imported into the Hama Fortran code. The parameters are listed as follow: 'r' range, 0-6 Å, k range, 0-12 Å<sup>-1</sup>; k weight, 2; and Morlet function with  $\kappa=5$ ,  $\sigma=2$  was used as the mother wavelet to provide the overall distribution.

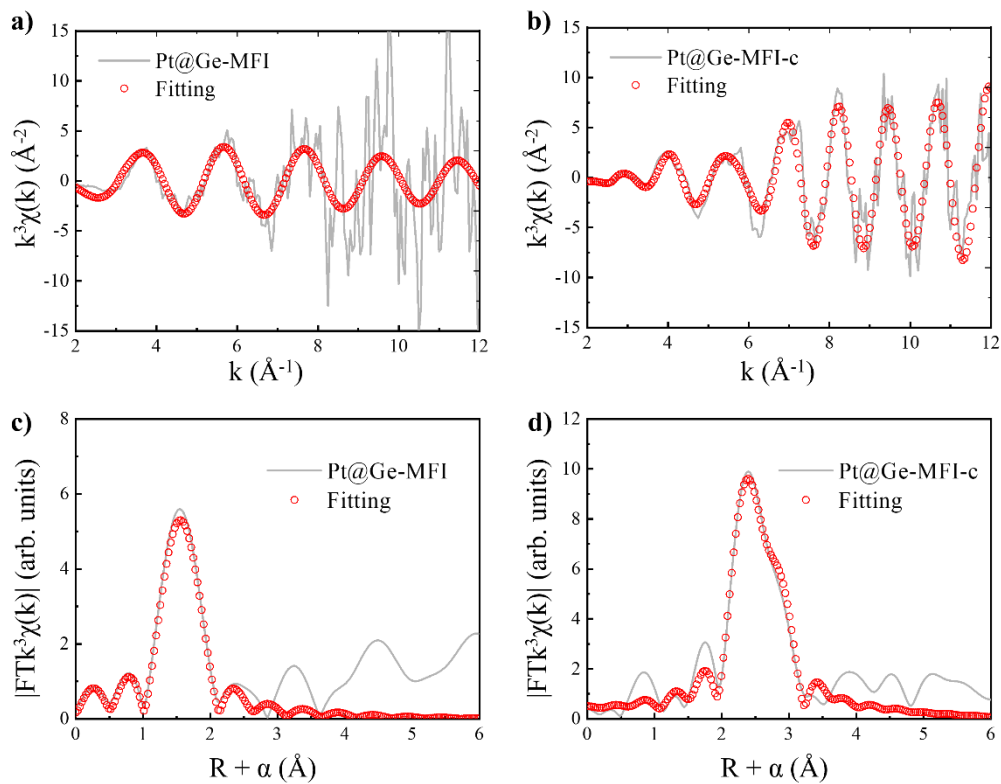


**Figure S9.**  $\chi(k)$  space spectra fitting curve of Pt@Ge-MFI (a) and Pt@Ge-MFI-c (b), and quantitative  $\chi(R)$  space spectra fitting curve of Pt@Ge-MFI (c) and Pt@Ge-MFI-c (d).

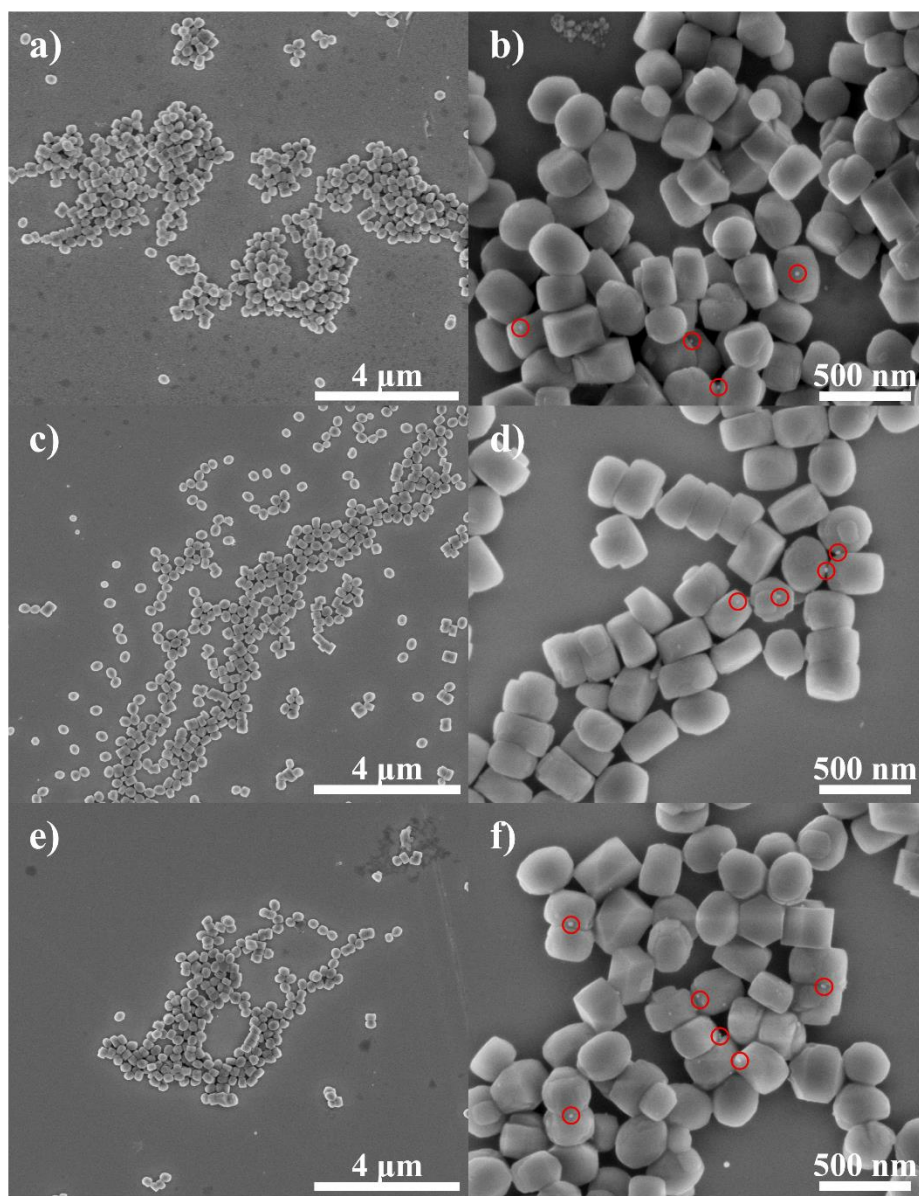


**Figure S10.** SEM images of Pt@Ge-MFI-c(r) (a-b), Pt@Ge-MFI-c (c-d) and Pt@Ge-MFI-c(s) (e-f), where 'r' refers to the raw sample without H<sub>2</sub> pre-reduction and 's' refers to the spent sample obtained after 12 hours' PDH reaction at 873K. Some of the Pt particles adhered to the zeolite surface are highlighted with red circles.

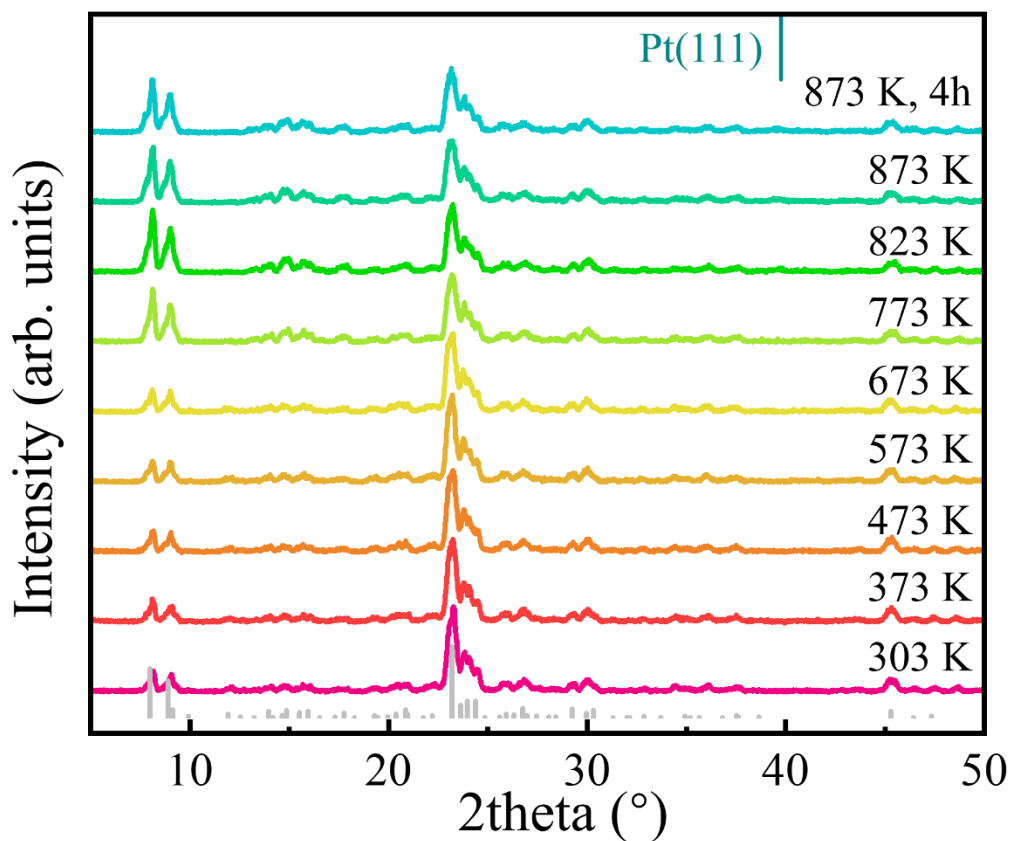


**Figure S11.** In-situ XRD patterns of Pt@Ge-MFI(r) during air calcination under increasing temperature, where 'r' refers to the raw sample without H<sub>2</sub> pre-reduction. The grey pattern is the standard pattern of Mutinaite (PDF#44-0002), an MFI-type mineral.

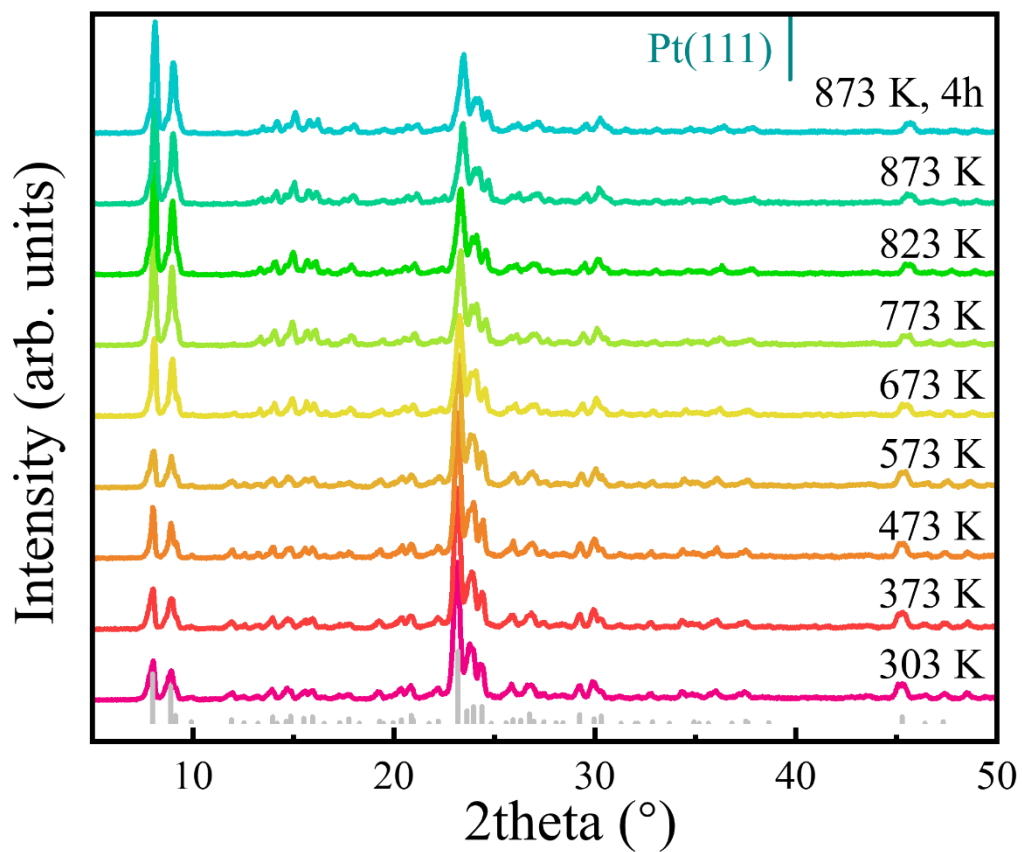


**Figure S12.** In-situ XRD patterns of Pt@Ge-MFI(r) during H<sub>2</sub> reduction under increasing temperatures, where r refers to the raw sample without H<sub>2</sub> pre-reduction or air calcination. The grey pattern is the standard pattern of Mutinaite (PDF#44-0002), an MFI-type mineral.

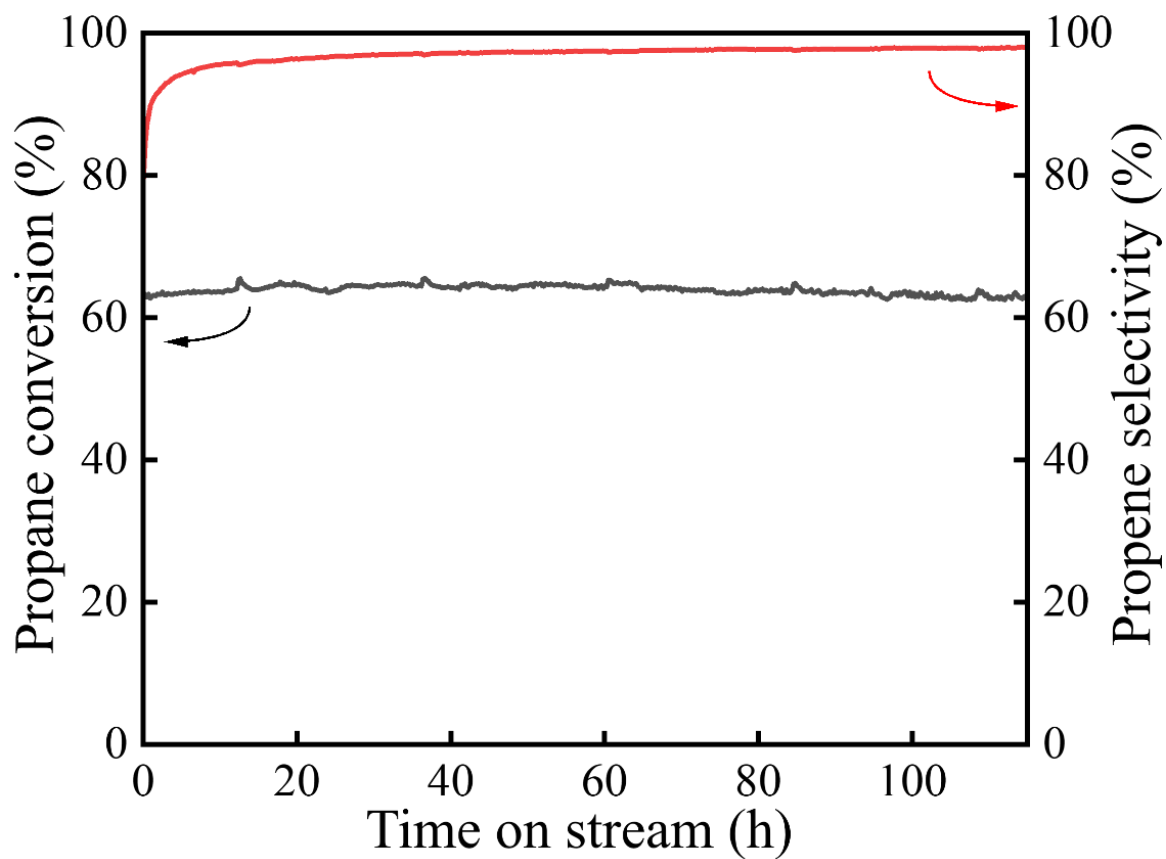


**Figure S13.** The catalytic performance of Pt@Ge-MFI under the condition of  $WHSV_{\text{propane}} = 1.75 \text{ h}^{-1}$ , propane/ $N_2 = 1/3$ , 873 K and atmospheric pressure.

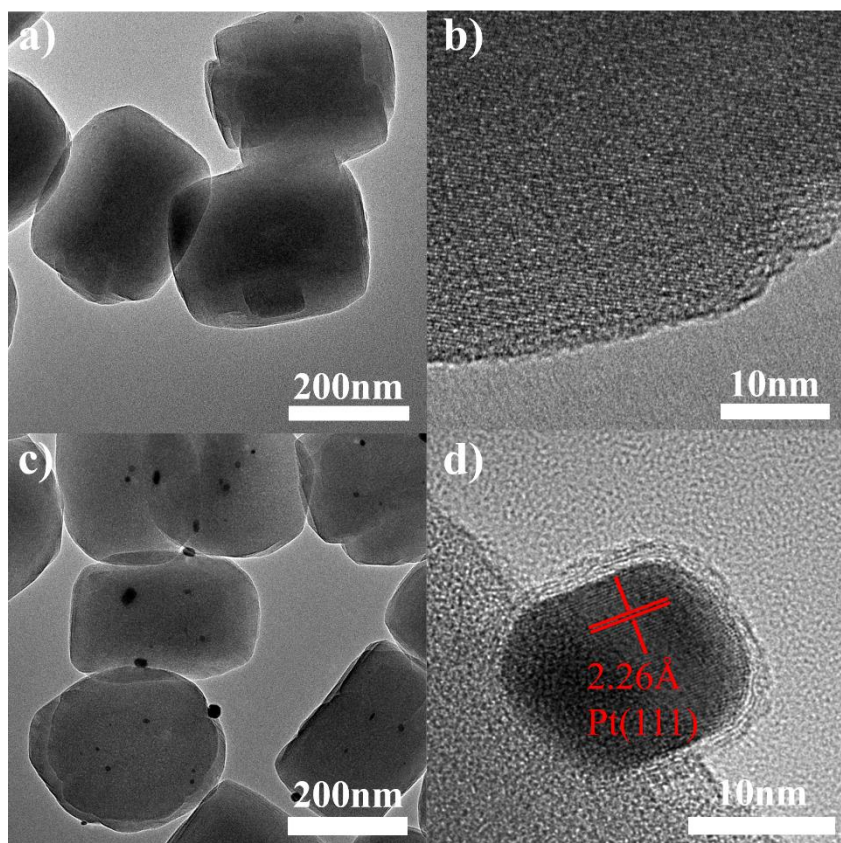


**Figure S14.** The TEM images of Pt@Ge-MFI(s) (a-b) and Pt@Ge-MFI-c(s) (c-d), where 's' refers to the spent sample obtained after 12 hours' PDH reaction at 873K.

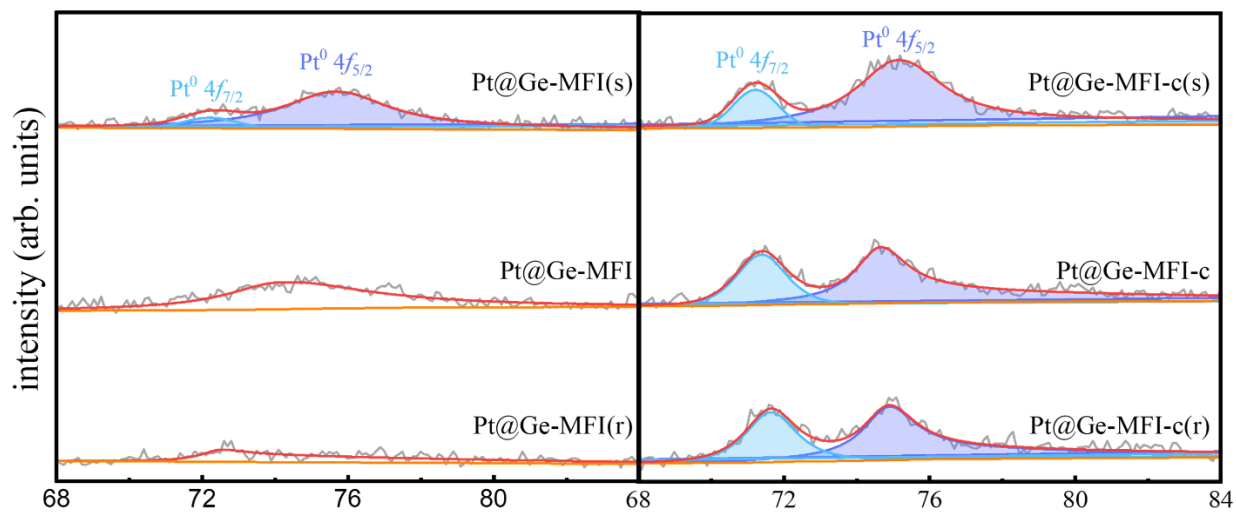


**Figure S15.** Pt 4f (b) XPS spectra of Pt@Ge-MFI catalysts, where 'r' refers to the raw sample without H<sub>2</sub> pre-reduction and 's' refers to the spent sample obtained after 12 hours' PDH reaction at 873K. The binding energy was calibrated using C 1s (284.8eV).

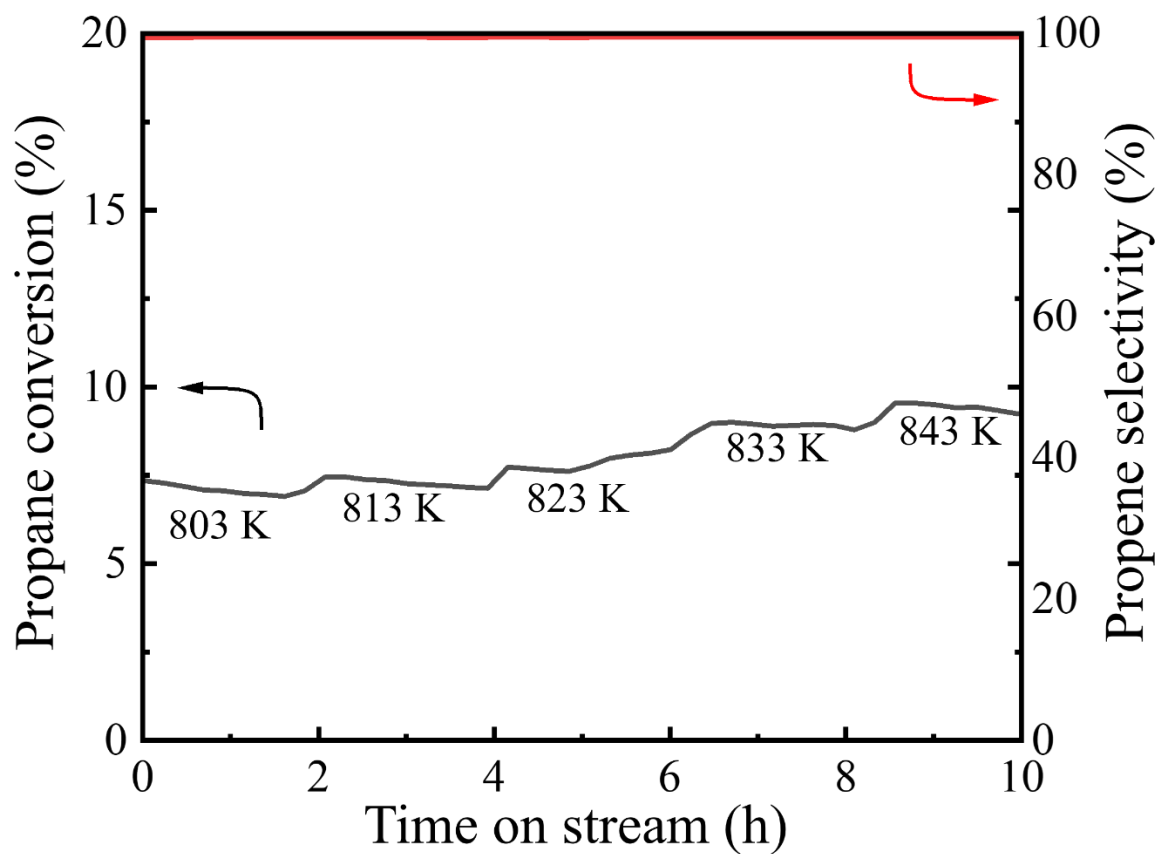


**Figure S16.** The catalytic performance of Pt@Ge-MFI at various temperatures as labeled in the figure.

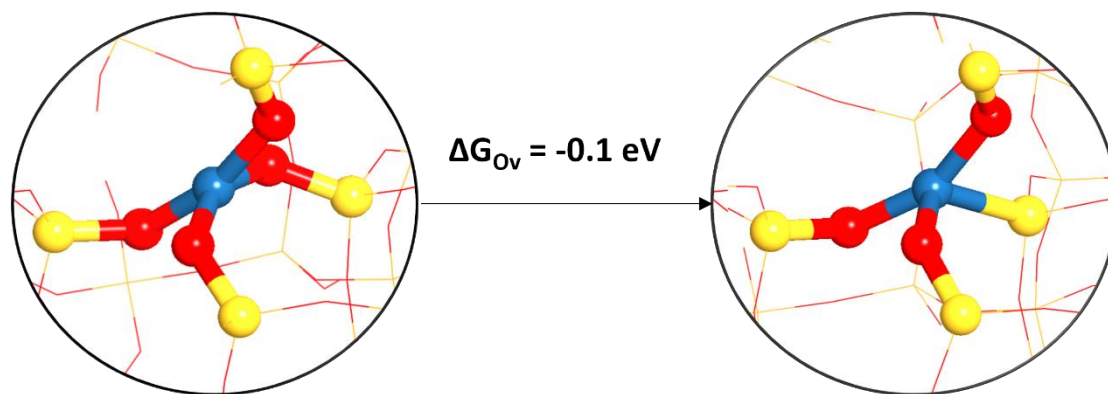


**Figure S17.** The scheme of oxygen removal of  $[\text{PtO}_4]$  in pure silica MFI zeolite framework.

## Supplementary References:

1. Lu, K. et al. Topotactic conversion of Ge-rich IWW zeolite into IPC-18 under mild condition. *Microporous and Mesoporous Materials* **310**(2021).
2. Zabinsky, S.I., Rehr, J.J., Ankudinov, A., Albers, R.C. & Eller, M.J. MULTIPLE-SCATTERING CALCULATIONS OF X-RAY-ABSORPTION SPECTRA. *Physical Review B* **52**, 2995-3009 (1995).
3. Ravel, B. & Newville, M. ATHENA, ARTEMIS, HEPHAESTUS: data analysis for X-ray absorption spectroscopy using IFEFFIT. *Journal of Synchrotron Radiation* **12**, 537-541 (2005).